Analyst

Determination of selenium in serum in the presence of gadolinium with ICP-QQQ-MS

David P. Bishop,†[a] Dominic J. Hare,†[a,b] Fred Fryer,[c] Regina V. Taudte,[a] Barbara R. Cardoso,[b,d] Nerida Cole[a] and Philip A. Doble*[a]

Gadolinium (Gd)-based magnetic resonance imaging (MRI) contrasting agents interfere with the determination of selenium (Se) when analysed by single quadrupole inductively coupled plasma-mass spectrometry (ICP-MS). This paper demonstrates that an ICP-triple quadrupole-MS (ICP-QQQ-MS) with oxygen mass shift overcomes Gd^{++} interference on Se^+ and mitigates typically encountered matrix and spectral based interferences. Normal human serum was diluted in a solution containing isopropanol, EDTA, NH_4OH and Triton X-100. Samples were unspiked (control) serum; serum spiked with 0.127 µmol L^{-1} Se or 127 µmol L^{-1} Gd; and serum spiked with both 0.127 µmol L^{-1} Se and 127 µmol L^{-1} Gd. Consideration of collision/reaction gases and conditions for interference mitigation included helium (He); a 'low' and 'high' hydrogen (H_2) flow, and oxygen (O_2). The instrument tune for O_2 was optimised for effective elimination of interferences *via* a mass shift reaction of Se^+ to SeO^+. The ICP-QQQ-MS was capable of detecting trace (>9.34 nmol L^{-1}) levels of Se in serum in the presence of Gd in our simulated post-MRI serum sample. The multi-tune capabilities of the ICP-QQQ-MS may be adapted to eliminate other specific isobaric interferences that cause false positive results in other analyses where the analyte is confounded by doubly charged and/or polyatomic species.

1. Introduction

Selenium (Se) is an essential trace element that is incorporated into the amino acid backbone of proteins as selenocysteine. Selenium has structural and enzymatic roles in 25 known human selenoproteins.[1–3] These proteins are antioxidants and required for the production of active thyroid hormone, but more recently roles in immune function, control of viruses such as HIV, prevention of cancer and reproductive health have been described.[4–9] Selenium deficiency has been associated with diseases affecting nutrient absorption including coeliac disease, some types of cancer, restricted diets and Keshan disease.[4,10–14] Additionally, a significant decline in blood Se levels with age has been reported.[15] Stated serum levels vary geographically. For example, in healthy European

populations levels ranged from around 0.5 to 1.2 µmol L^{-1} of Se.[15–17] while levels as low as 0.34 µmol L^{-1} have been reported in populations where Keshan disease occurs.[18]

Single quadrupole inductively coupled plasma-mass spectrometry (SQ-ICP-MS) is the preferred standard analytical method for analysis of most elements in biological fluids, and represents 95% of all commercial ICP-MS instruments.[19] The two most abundant isotopes are ^{80}Se and ^{78}Se, with ^{82}Se the preferred isotope for pre-collision cell technology along with interference equation correction, due to less isobaric interferences from the argon plasma and the sample matrix (Table 1),

[a]*Elemental Bio-imaging Facility, University of Technology Sydney, Broadway, New South Wales 2007, Australia. E-mail: philip.doble@uts.edu.au; Fax: +61 2 9514 1460; Tel: +61 2 9514 1792*
[b]*The Florey Institute of Neuroscience and Mental Health, The University of Melbourne, Parkville, Victoria, Australia*
[c]*Agilent Technologies, Mulgrave, Victoria, Australia*
[d]*Faculty of Pharmaceutical Sciences, Department of Food and Experimental Nutrition, University of São Paolo, Brazil*
† Equal first authors.

Table 1 Target Se isotopes and potential interferences. Adapted from May and Wiedmeyer[29]

Isotope	Natural abundance (%)	Potential molecular interferences
^{74}Se	0.89	$^{37}Cl_2^+$, $^{36}Ar^{38}Ar^+$, $^{38}Ar^{36}S^+$, $^{40}Ar^{34}S^+$
^{76}Se	9.37	$^{40}Ar^{36}Ar^+$, $^{38}Ar_2^+$
^{77}Se	7.63	$^{40}Ar^{37}Cl^+$, $^{36}Ar^{40}Ar^1H^+$, $^{38}Ar_2^1H^+$, $^{12}C^{19}F^{14}N^{16}O_2^+$, $^{154}Gd^{++}$, $^{155}Gd^{++}$ spread
^{78}Se	23.8	$^{40}Ar^{38}Ar^+$, $^{38}Ar^{40}Ca^+$, $^{78}Kr^+$, $^{156}Gd^{++}$, $^{157}Gd^{++}$ spread
^{80}Se	49.6	$^{40}Ar_2^+$, $^{32}S^{16}O_3^+$, $^{79}Br^1H^+$, $^{80}Kr^+$, $^{160}Gd^{++}$
^{82}Se	8.73	$^{12}C^{35}Cl_2^+$, $^{34}S^{16}O_3^+$, $^{40}Ar_2^1H_2^+$ $^{81}Br^1H^+$, $^{82}Kr^+$

whilst [78]Se is the preferred isotope when using collision cells. Gadolinium (Gd) is widely used in contrasting agents for magnetic resonance imaging (MRI) of the vasculature and tumours of the central nervous system,[20] and interferes with the major isotopes of Se due to doubly charged Gd species.[21–23]

Consequently, incorrect diagnosis of Se toxicity may arise from the presence of high levels of circulating Gd. Total elimination of circulating Gd may be in the order of days or longer for those with impaired renal function.[24] For example, in 2008, a clinical urine sample measured by ICP-MS returned a Se concentration of 16.8 µmol L^{-1}, a level associated with acute Se poisoning. This measurement was an artefact resulting from an MRI procedure performed on the day of testing using a Gd contrasting agent.[22]

Interference on Se is typically managed by a collision/reaction cell which removes polyatomic species with kinetic energy discrimination or by chemically induced dissociation, providing reduced backgrounds and improved limits of detection and quantification.[21,25] The higher mass resolving power of double-focusing sector field mass-spectrometers (ICP-SF-MS) is an alternative to reducing the impact of polyatomic and isobaric interferences on mass measurements.[26–28] However, ICP-SF-MS are costly, complex, and high resolution settings compromise the sensitivity of the analysis when resolving Ar dimers from Se. Comparisons of SQ-ICP-MS with a collision/reaction cell against a SF-ICP-MS demonstrated that [80]Se$^+$ could not be resolved from [40]Ar$_2$$^+$ in the high-resolution SF-ICP-MS and the SQ-ICP-MS had superior isotope ratio precision and a lower LOD.[30] Mathematical corrections may also be used to remove the signal from doubly charged[31] and polyatomic species,[32] but are less accurate than removing interfering species by physical methods.

The triple quadrupole ICP-MS (ICP-QQQ-MS) reduces interferences by operating in either standard single quadrupole (SQ) mode or tandem MS/MS. In the MS/MS mode a quadrupole (Q1) filters the mass-to-charge ratio (m/z) of interest prior to introduction into an ion-guide (Q2), which has the option to be filled with a collision and/or reaction gas. The final quadrupole (Q3) again filters the desired analyte, either on its original mass or the known reaction product.[33] O$_2$ may be used to react with kinetically favoured analytes to an MO$^+$ mass filtered by Q3, removing all other interfering species. This approach was applied to the measurement of selenoproteins in rat serum by liquid chromatography (LC)-ICP-MS/MS[34] and arsenic (As) and Se in food.[35] This MO$^+$ mass shift improved detection limits for phosphorus (P), sulfur (S) and silicon (Si) over those obtained from isotope dilution (ID)-ICP-SF-MS in both aqueous[34] and organic matrices.[34,36] However if O$_2$ reaction has the potential to produce unwanted polyatomic species; then alternative reaction/collision gases may be used, e.g. NH$_3$/He for the ultra-trace detection of titanium (Ti; as Ti(NH$_3$)$_6$$^+$) in biological fluids.[37]

This paper describes the analysis of clinically relevant concentrations of Se in serum samples in the presence of Gd via an O$_2$ mass shift approach.

2. Experimental

2.1 Instrumentation

All analyses were performed using an Agilent Technologies 8800 Series ICP-QQQ-MS (Mulgrave, Victoria, Australia). Four tune modes were evaluated; (tune mode 1) high energy helium (HE-He), 10 mL min^{-1} He flow; (tune mode 2) H$_2$ at a low cell flow (low H$_2$), 5 mL min^{-1} H$_2$ flow; (tune mode 3) high flow H$_2$ (high H$_2$), 9 mL min^{-1} H$_2$ flow; and (tune mode 4) O$_2$, 0.28 mL min^{-1} O$_2$ flow. Gd (m/z = 156, 157) was measured on mass for tune modes 1–3, Se m/z 77 and 78 were analysed for the HE-He tune, and Se m/z 77, 78 and 82 for the two H$_2$ tune modes. The elements were measured with a [16]O mass shift with the O$_2$ tune (m/z 77 → 93, 78 → 94, 80 → 96, 82 → 98, 156 → 172, 157 → 173). The octopole bias (OctP Bias) and the energy discrimination were optimised for each tune mode (see Table 2).

2.2 Reagents

Human serum, A.C.S.-grade EDTA-acid, Triton X-100 and NH$_4$OH were obtained from Sigma Aldrich (Castle Hill, New South Wales, Australia). HPLC-grade isopropanol was purchased from Chem-Supply (Gilman, South Australia, Australia), 99.999% purity O$_2$, He, and H$_2$ from BOC (North Ryde, New South Wales, Australia), and high purity Se, Gd and tellurium (Te) standards from Choice Analytical (Thornleigh, New South Wales, Australia).

2.3 Sample preparation

Sample preparation was modified from that described by Burri and Haldimann.[38] Briefly, a diluent containing 4% isopropanol, 0.1% EDTA, 0.1% Triton X-100 and 2% NH$_4$OH was prepared. Te was added to this solution as the internal standard to a final concentration of 0.130 µmol L^{-1} in the sample. 0.25 mL of serum was mixed with 2.5 mL of diluent, with the volume made to 5.0 mL with MilliQ water and element (Se/Gd) spike. Samples were spiked with an appropriate amount of Se to give a concentration of 0.127 µmol L^{-1}, and Gd spiked at a concentration of 127 µmol L^{-1} (based on post-MRI serum Gd values reported by Brown et al.[39]). Four sample groups of 10 replicates each were prepared; a serum blank, Se, Gd, and Se + Gd spiked sample. The concentration of Se in our serum samples (0.127 µmol L^{-1}) represented both Se-deficient adult or low-range infant serum Se concentrations.[40]

2.4 Data analysis

Following instrument calibration by standard addition, sample concentrations for each m/z in the 10 replicate samples was

Table 2 ICP-QQQ-MS collision/reaction cell parameters

Tune mode	Cell gas flow	OctP bias (V)	Energy discrimination (V)	ICP mode
HE-He	10 mL min^{-1}	−100	7	SQ
Low H$_2$	5.0 mL min^{-1}	−18	1.5	MS/MS
High H$_2$	9.0 mL min^{-1}	−18	1.5	MS/MS
O$_2$	0.28 mL min^{-1}	−3	−5	MS/MS

calculated using the Agilent ICP-MS MassHunter data analysis software. Statistical analysis (Student's t-test; $p < 0.05$) was performed in Prism 6 (GraphPad, La Jolla, California, United States of America).

3. Results

3.1 Collision/reaction conditions

Four tune modes were examined for the determination of Se in human serum under conditions simulating those following the administration of a Gd MRI contrasting agent. The modes represented three commonly used methods of interference removal; kinetic energy discrimination (He), removal *via* reaction with hydrogen (H_2), or adduct formation *via* reaction with O_2.

For tune mode 1, Q1 was set as an ion guide. Tune 1 (HE-He) used a high potential difference (the OctP bias) to accelerate incoming ions into the He-filled octopole cell for collisional induced dissociation of the ArAr dimer. Energy discrimination was optimised to reduce ions escaping the confines of the cell maintaining a low background. For tunes 2 and 3 (H_2 tunes) the cell was optimised for *reaction mode*. To facilitate desirable in-cell reactions, a low negative voltage OctP bias accelerated ions into the cell, and a slight positive bias limited in-cell products from exiting the cell, providing more time for reaction. Tune mode 2 used an H_2 flow rate of 5.0 mL min^{-1} (standard conditions for Se determination, to reduce the $^{40}Ar^{38}Ar^+$ dimer at m/z 78), and tune mode 3 used a higher flow rate (9.0 mL min^{-1}), determined experimentally as the optimal rate to reduce $^{156}Gd^{++}$ interference on m/z 78, whilst maintaining adequate sensitivity for $^{78}Se^+$ (Fig. 1). In the case of tune mode 4 (O_2 mass shift), the energy and cell gas flow was optimised to maximise the low yield endothermic $Se^+ + O \rightarrow SeO^+$ reaction (δ 0.69 eV), and to minimise the exothermic reaction of Gd^{++} with O_2 ($Gd^+ + O \rightarrow GdO^+$, δ −2.39 eV). Energy discrimination of −5 V was experimentally determined to minimise $^{156}Gd^{16}O_2^{++}$ and maximise $^{78}Se^{16}O^+$ passage through the collision/reaction cell and into Q3. The first mass filter (Q1) limited the transmission to the cell of plasma generated ions to the selected mass. The results are shown in Table 3.

3.2 Instrument performance

The amount of Se spiked into the serum standard was selected from typical ranges reported by Thomson.[41] The limits of detection (LOD) and quantification (LOQ) (Table 4) were determined from the signal intensities using eqn (1), where $y = 3$ for LOD and 10 for LOQ.

$$\text{Limit} = y \left(\frac{\text{SD[blank]}}{(\text{mean[spikes]} - \text{mean[blanks]})} \times \text{spike concentration} \right) \tag{1}$$

LOD and LOQ data were not acquired for ^{80}Se for tune modes 1–3 due to inability of the ICP-QQQ-MS to discriminate m/z 80 for $^{80}Se^+$ and $^{40}Ar_2^+$. Tune mode 4 permitted the monitoring of the $^{80}Se^+$ isotope as $^{80}Se^{16}O^+$.
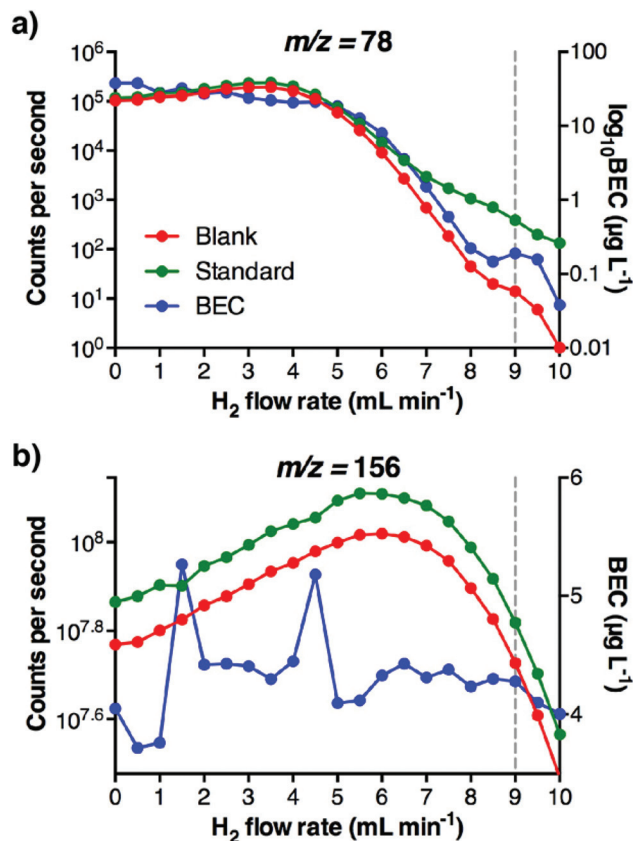

Fig. 1 High H_2 flow rate performance: ramp cell gas plots for high H_2 (tune mode 3) reaction with m/z = 78 (a) and 156 (b). BEC = background equivalent concentration. Dashed grey line denotes selected H_2 flow rate that maximises the signal of m/z 78 above the blank while reducing the signal of m/z 156. Blank contains 127 µmol L^{-1} Gd in serum, standard is 0.127 µmol L^{-1} Se in 127 µmol L^{-1} Gd in serum. At 9 mL min^{-1} H_2 (dashed grey line) there is the greatest difference between the blank and the standard, while maintaining sufficient signal strength.

4. Discussion

The isotopes of Se that may be determined are shown in Table 1. The most commonly measured isotope is ^{78}Se (23.8% NA), graphically represented in Fig. 2a–d for each tune mode. The presence of the Gd^{++} interference was not mitigated by the HE-He tune (tune mode 1), the low H_2 tune (tune mode 2), or the high flow H_2 tune (tune mode 3), with Se concentrations overestimated by up to 20 times. The O_2-induced mass shift using tune mode 4 sufficiently removed doubly-charged Gd interference, which also allowed measurement of the more highly-abundant ^{80}Se isotope by shifting the measured m/z away from the $^{40}Ar_2^+$ interference (Fig. 2e). The O_2 mass shift (tune mode 4) was clearly the most accurate and precise method with recoveries of 99.7–101.8% for ^{77}Se, ^{78}Se, ^{80}Se and ^{82}Se from Se + Gd spiked serum samples.

Helium is often used as a collision gas to reduce interferences on the majority of elements. Tune mode 1 (HE-He) removed the ArAr interference on $^{77,78}Se^+$, however it did not eliminate the $^{154,156}Gd^{++}$ signal. This tune did not remove the

Table 3 Concentration of Se (± 1 standard deviation) in samples per tune mode ($\mu mol\ L^{-1}$)

	Serum blank	Gd	Se	Se + Gd
^{77}Se HE-He	0.0524 ± 0.0065	8.78 ± 0.58	0.166 ± 0.008	8.96 ± 0.39
^{78}Se HE-He	0.0528 ± 0.0061	32.6 ± 2.2	0.168 ± 0.007	32.8 ± 1.3
^{77}Se Low H$_2$	0.0405 ± 0.0051	0.546 ± 0.009	0.134 ± 0.009	0.627 ± 0.014
^{78}Se Low H$_2$	0.0445 ± 0.0046	0.546 ± 0.029	0.146 ± 0.008	0.627 ± 0.023
^{82}Se Low H$_2$	0.0506 ± 0.0050	0.0578 ± 0.0053	0.161 ± 0.009	0.171 ± 0.010
^{77}Se High H$_2$	0.0501 ± 0.0043	0.0631 ± 0.0052	0.159 ± 0.010	0.174 ± 0.011
^{78}Se High H$_2$	0.0478 ± 0.0046	0.0526 ± 0.0049	0.151 ± 0.010	0.158 ± 0.011
^{82}Se High H$_2$	0.0478 ± 0.0046	0.0526 ± 0.0055	0.151 ± 0.009	0.158 ± 0.009
^{77}Se O$_2$	0.0534 ± 0.0050	0.0581 ± 0.0056	0.170 ± 0.011	0.169 ± 0.010
^{78}Se O$_2$	0.0532 ± 0.0047	0.0604 ± 0.0052	0.168 ± 0.012	0.171 ± 0.010
^{80}Se O$_2$	0.0520 ± 0.0045	0.0576 ± 0.0054	0.165 ± 0.010	0.166 ± 0.009
^{82}Se O$_2$	0.0517 ± 0.0045	0.0546 ± 0.0053	0.163 ± 0.010	0.162 ± 0.009

Table 4 Limits of analysis ($\mu mol\ L^{-1}$) for each tune mode

|		HE-He	Low H$_2$	High H$_2$	O$_2$
^{77}Se	LOD	0.00945	0.00982	0.00944	0.0102
	LOQ	0.0315	0.0327	0.0314	0.0341
^{78}Se	LOD	0.0111	0.0108	0.00954	0.0107
	LOQ	0.0370	0.0360	0.0318	0.0336
^{80}Se	LOD	NM^a	NM	NM	0.00934
	LOQ	NM	NM	NM	0.0311
^{82}Se	LOD	NM	NM	0.01360	0.0107	0.00965
	LOQ	NM	NM	0.04540	0.0359	0.0322

^{a} NM = not measured.

$^{40}Ar^{40}Ar^+$ interference on $^{80}Se^+$, whilst $^{82}Se^+$ was not examined due to the high number of polyatomic interferences arising from the biological matrix (Table 1).

Tune mode 2 (low H$_2$) effectively removed the polyatomic interferences, but was unable to sufficiently reduce the interference caused by the Gd^{++} ions. Tune mode 3 (high H$_2$) mitigated the polyatomic interferences on $^{77,78,82}Se^+$ and eliminated the $^{154}Gd^{++}$ (NA 2.18%) interference on $^{77}Se^+$ ($p < 0.05$).

Tune mode 3 failed to eliminate the $^{156}Gd^{++}$ (NA 20.5%) interference on $^{78}Se^+$. This contrasts with Harrington et al.[21] who found that H$_2$ in the collision cell with a flow rate of 3.26 mL min^{-1} removed Gd^{++} interference on the Se signal in serum due to the concentration of Se an order of magnitude higher than this study (0.127 $\mu mol\ L^{-1}$ vs. 1.01–3.56 $\mu mol\ L^{-1}$). Similarly, Jackson et al.[35] removed the interference of $^{156}Gd^{++}$ on the measurement of $^{78}Se^+$ with a H$_2$ cell gas flow of 6 mL min^{-1} in food samples, also due to high to relatively high concentrations of Se; and a Gd spike 200 times lower than our simulation of post-MRI serum Gd concentration.

Other concerns with H$_2$ as a reaction gas include patients with high levels of circulating bromine, arising from bromhexine hydrochloride, a common ingredient in expectorants. H$_2$ reacts with $^{79}Br^+$ and $^{81}Br^+$ to form isobaric interferences on $^{80}Se^+$ and $^{82}Se^+$, respectively. Deuterium has been used to overcome BrH$^+$ interferences,[42] though high expense limits its practical usage.

Tune mode 4 maximised the formation of Se^{16}O$^+$ adducts and minimised the influence of doubly-charged Gd species on Se detection across all isotopes and was the superior method for Se determination, irrespective of isotope. Others have
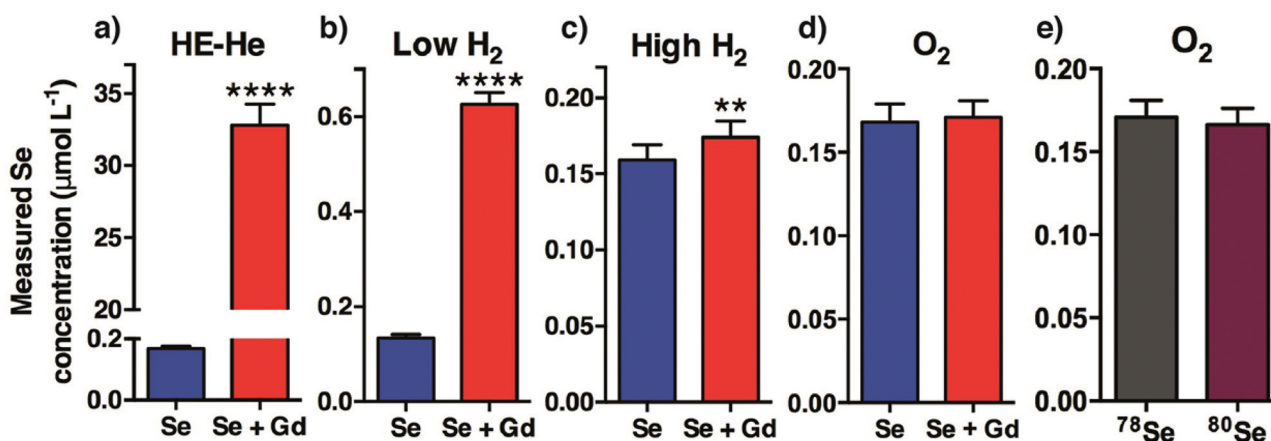
Fig. 2 Gd^{++} interference removal efficiency: comparison of measured Se concentrations of Se spiked (blue) and Se + Gd spiked (red) samples. HE-He (a; tune mode 1), low H$_2$ (b; tune mode 2) and high H$_2$ (c; tune mode 3) were all unable to sufficiently remove $^{156}Gd^{++}$ interference on $^{78}Se^+$ (****$p < 0.0001$; **$p < 0.01$; $n = 10$). Measuring the mass shift of 78→94 ($^{78}Se^{16}O^+$) resulting from reaction with O$_2$ (d; tune mode 4) was able to adequately remove $^{156}Gd^{++}$ interference ($p = 0.535$; $n = 10$). Furthermore, O$_2$ mass shift permitted analysis of the higher NA isotope ^{80}Se (NA 49.6%), with no significant difference in measured Se concentration observed between measured $^{78}Se^{16}O^+$ and $^{80}Se^{16}O^+$ masses (e; $p = 0.316$; $n = 10$).

increased the yield of SeO^+ with mixed gases of H_2 and O_2 in the collision cell.[35] We also trialled mixed cell gases and did not observe any benefit.

Minimising unwanted masses entering, and preventing undesirable interactions, in the collision cell, is a significant feature of the ICP-QQQ-MS. For example S^+ may be removed from the ion path before it reaches the collision cell, where it could potentially form kinetically favourable species such as $^{32}S^{16}O_3^+$. The ICP-QQQ-MS may also find application in method validation strategies by ensuring isotopically pure signals particularly for analytes known to be confounded by polyatomic or isobaric interferences.

5. Conclusions

Gd-based MRI contrasting agents interfere with Se analyses by ICP-MS. Reaction with O_2 using the ICP-QQQ-MS allowed a mass shift reaction of Se, which enabled detection of all major isotopes of Se with adequate sensitivity in the presence of Gd. Additionally, this approach overcame interferences from Ar dimers, further improving the sensitivity of the analysis. ICP-QQQ-MS has the unique capability to selectively isolate ions of interest from interferences or confounding signals at low concentrations, as demonstrated in this simulated scenario of Gd interference on serum Se levels.

Notes and references

1 G. V. Kryukov, *Science*, 2003, **300**, 1439–1443.
2 S. J. Fairweather-Tait, Y. Bao, M. R. Broadley, R. Collings, D. Ford, J. E. Hesketh and R. Hurst, *Antioxid. Redox Signaling*, 2011, **14**, 1337–1383.
3 K. M. Brown and J. R. Arthur, *Public Health Nutr.*, 2007, 4.
4 D. L. Hatfield, P. A. Tsuji, B. A. Carlson and V. N. Gladyshev, *Trends Biochem. Sci.*, 2014, **39**, 112–120.
5 I. L. Heras, M. Palomo and Y. Madrid, *Anal. Bioanal. Chem.*, 2011, **400**, 1717–1727.
6 M. Roman, P. Jitaru, M. Agostini, G. Cozzi, S. Pucciarelli, D. Nitti, C. Bedin and C. Barbante, *Microchem. J.*, 2012, **105**, 124–132.
7 J. Salonen, G. Alfthan, J. Huttunen, J. Pikkarainen and P. Puska, *Lancet*, 1982, **320**, 175–179.
8 G. N. Schrauzer, D. A. White and C. J. Schneider, *Bioinorg. Chem.*, 1977, **7**, 23–34.
9 G. N. Schrauzer, D. A. White and C. J. Schneider, *Bioinorg. Chem.*, 1978, **8**, 387–396.
10 T. D. Shultz and J. E. Leklem, *Am. J. Clin. Nutr.*, 1983, **37**, 114–118.
11 P. Collin, K. Kaukinen, M. Välimäki and J. Salmi, *Endocr. Rev.*, 2002, **23**, 464–483.
12 I. Hafström, B. Ringertz, A. Spångberg, L. von Zweigbergk, S. Brannemark, I. Nylander, J. Rönnelid, L. Laasonen and L. Klareskog, *Rheumatology*, 2001, **40**, 1175–1179.
13 M. A. Reeves and P. R. Hoffmann, *Cell. Mol. Life Sci.*, 2009, **66**, 2457.
14 J. Loscalzo, *N. Engl. J. Med.*, 2014, **370**, 1756–1760.
15 S. Letsiou, T. Nomikos, D. Panagiotakos, S. Pergantis, E. Fragopoulou, S. Antonopoulou, C. Pitsavos and C. Stefanadis, *Biol. Trace Elem. Res.*, 2009, **128**, 8–17.
16 M. P. Rayman, *Lancet*, 2000, **356**, 233–241.
17 M. Rükgauer, J. Klein and J. D. Kruse-Jarres, *J. Trace Elem. Med. Biol.*, 1997, **11**, 92–98.
18 A. T. Diplock, *Am. J. Clin. Nutr.*, 1993, **57**, 256S–258S.
19 D. Potter, *J. Anal. At. Spectrom.*, 2008, **23**, 690–693.
20 J. M. Idee, M. Port, I. Raynal, M. Schaefer, S. Le Greneur and C. Corot, *Fundam. Clin. Pharmacol.*, 2006, **20**, 563–576.
21 C. F. Harrington, A. Walter, S. Nelms and A. Taylor, *Ann. Clin. Biochem.*, 2014, **51**, 386–391.
22 A. Walter, S. Nelms, C. F. Harrington and A. Taylor, *Ann. Clin. Biochem.*, 2011, **48**, 176–177.
23 A. J. Steuerwald, P. J. Parsons, J. G. Arnason, Z. Chen, C. M. Peterson and G. M. B. Louis, *J. Anal. At. Spectrom.*, 2013, **28**, 821–830.
24 S. Aime and P. Caravan, *J. Magn. Reson. Imaging*, 2009, **30**, 1259–1267.
25 L. Hinojosa Reyes, J. M. Marchante-Gayon, J. I. Garcia Alonson and A. Sanz-Medel, *J. Anal. At. Spectrom.*, 2003, **18**, 11–16.
26 A. M. Featherstone, A. T. Townsend, G. A. Jacobson and G. M. Peterson, *Anal. Chim. Acta*, 2004, **512**, 319–327.
27 C. S. Muniz, J. M. Larchante-Gayon, J. I. G. Alonso and A. Sanz-Medel, *J. Anal. At. Spectrom.*, 1999, **14**, 193–198.
28 G. A. Jacobson, Y. C. Tong, A. T. Townsend, A. M. Featherstone, M. Ball, I. K. Robertson and G. M. Peterson, *Eur. J. Clin. Nutr.*, 2007, **61**, 1057–1063.
29 T. W. May and R. H. Wiedmeyer, *At. Spectrosc.*, 1998, **19**, 150–155.
30 N. Elwaer and H. Hintelmann, *Talanta*, 2008, **75**, 205–214.
31 A. L. Gray and J. G. Williams, *J. Anal. At. Spectrom.*, 1987, **2**, 81–82.
32 J. Goossens, L. Moens and R. Dams, *Talanta*, 1994, **41**, 187–193.
33 L. Balcaen, G. Woods, M. Resano and F. Vanhaecke, *J. Anal. At. Spectrom.*, 2013, **28**, 33.
34 Y. Anan, Y. Hatakeyama, M. Tokumoto and Y. Ogra, *Anal. Sci.*, 2013, **29**, 787–792.
35 B. P. Jackson, A. Liba and J. Nelson, *J. Anal. Atom. Spectrom.*, 2015, DOI: 10.1039/C4JA00310A.
36 R. S. Amais, C. D. B. Amaral, L. L. Fialho, D. Schiavo and J. A. Nóbrega, *Anal. Methods*, 2014, **6**, 4516–4520.
37 L. Balcaen, E. Bolea-Fernandez, M. Resano and F. Vanhaecke, *Anal. Chim. Acta*, 2014, **809**, 1–8.
38 J. Burri and M. Haldimann, *Clin. Chem. Lab. Med.*, 2007, **45**, 895–898.
39 J. J. Brown, M. R. Hynes, J. Wible and J. H, *Am. J. Roentgenol.*, 2007, **189**, 1539–1544.
40 A. C. Muntau, M. Streiter, M. Kappler, W. Röschinger, I. Schmid, A. Rehnert, P. Schramel and A. A. Roscher, *Clin. Chem.*, 2002, **48**, 555–560.
41 C. D. Thomson, *Eur. J. Clin. Nutr.*, 2004, **58**, 391–402.
42 Y. Ogra, K. Ishiwata and K. T. Suzuki, *Anal. Chim. Acta*, 2005, **554**, 123–129.